

Evidence of a Surface Acceptor State in Undoped Semi-Insulating GaAs by Photothermal Radiometric Deep Level Transient Spectroscopy

Andreas Mandelis** and R. Arief Budiman
*Photothermal and Optoelectronic Diagnostics Laboratories,
 Department of Mechanical and Industrial Engineering,
 University of Toronto, Toronto, Ontario M5S 3G8, Canada*

Siloxane passivated, undoped semi-insulating GaAs samples exhibit a smaller emission time constant in photothermal radiometric signal decay than untreated samples. Surface photovoltage and photoluminescence results for the passivated sample indicate an upwards surface band bending which induces hole accumulation on the sample surface. This will decrease the hole emission rate from a surface acceptor located at $E_V + 0.27$ eV. We also detected an identical activation energy in the untreated samples, which verifies the energetic location of the acceptor state. The thermal emission cross section determined for this acceptor strongly correlates with a discrete-surface-state model rather than a continuum-surface-state model, and helps explain Fermi level pinning in GaAs.

** To whom correspondence should be address; electronic mail: mandelis@mie.utoronto.ca

Introduction

In this paper, we report on the first experimental evidence of a surface acceptor state in semi-insulating GaAs from photothermal radiometric deep-level transient spectroscopy (PTR-DLTS) spectra. In conventional deep level impurity characterization techniques, such as capacitance deep-level transient spectroscopy (DLTS), this state cannot be detected, because of its energetic location with respect to the barrier height. While the barrier heights in GaAs vary between 0.6 eV to 1.1 eV¹, the surface acceptor state we have observed is located at 0.27 eV above valence band maximum.

The significance of this surface state lies in the fact that it helps shed more understanding to Fermi level pinning at GaAs interfaces. At the device level this effect creates a dominant, undesirable nonradiative recombination path for GaAs-based laser structures and undoped semi-insulating GaAs substrates. Researchers have tried to understand its physical mechanisms by offering various models, notably the advanced unified defect mode (AUDM) by Spicer *et al.*², the unified disorder induced gap state (DIGS) model by Hasegawa and Ohno³, and the metal-induced gap state (MIGS) model by Tersoff⁴. Both the AUDM and the DIGS models have confirmed from their independent experimental results that Fermi level pinning largely originates from the electronic structure of the host semiconductor crystal, when a metal-semiconductor junction is formed. In GaAs-based devices this often means undoped semi-insulating GaAs. Nonetheless, the initial electronic configuration of the semi-insulating GaAs is often discussed. The MIGS model, on the other hand, maintains that the metal will dominate over the substrate in pinning the Fermi level. To determine which model realistically explains the situation in undoped semi-insulating GaAs, we only need to prove the existence of a surface acceptor state on this substrate. However, this state has not been experimentally verified, although it was postulated by the AUDM and the DIGS models to account for a compensation mechanism with a surface donor state which is often linked to the bulk EL2 level since both

occupy similar energetic locations. The main reason for this lack of information stems from the limitations of conventional capacitance DLTS which makes use of a Schottky or ohmic contact. Both of these contacts fail to produce a detectable signal from semi-insulating GaAs substrates due to the extended space charge layer width of these substrates. More importantly, both contacts will most likely introduce metal-induced gap states⁵ and energetically bury the acceptor state below the barrier height. Similar situations will arise for the conventional transient spectroscopic techniques^{6,7} due to their requirements for electrical contacts, even though those techniques were originally specifically designed for semi-insulating substrates.

Experimental

Recently, we introduced photothermal radiometric deep level transient spectroscopy (PTR-DLTS)⁸ in order to eliminate all electrical contacts to the sample. This allows the observation of both capture and emission processes from surface states in a noncontact manner by using above bandgap light as an excitation source. PTR-DLTS detects time-dependent infrared emission in the wavelength regime of $\lambda = 2\text{-}14$ μm due to free carrier de-excitation in the sample, which indirectly relates to the evolution of the depth-integrated excess carrier population.

The PTR-DLTS setup used in this study has been discussed elsewhere.^{8,9} It is worthwhile, however, to mention that we maintain the rate window detection technique that is used in capacitance DLTS to produce a PTR-DLTS spectrum with temperature as the independent variable. A peak is produced in the spectrum when the pulse repetition period of the optical pump matches the time constant in the PTR-DLTS signal decay, which is subsequently processed by a two-phase lock-in amplifier. Thus, by varying the pulse repetition periods, several peaks will be produced at different temperatures. From these peaks, the dependence of the time constant on the

temperature is obtained, which will give the activation energy of the deep level impurity:

$$\tau \sim T_o = \frac{I}{\sigma_p N_V v_{th,p}} \exp\left[\frac{\Delta E}{kT}\right] = \frac{\text{constant}}{T^2} \exp\left[\frac{\Delta E}{kT}\right], \quad (1)$$

where T_o and ΔE are pulse repetition period and activation energy, respectively. The three material parameters are: capture cross section σ_p , effective density of states in valence band N_V , and thermal velocity of carriers $v_{th,p}$. An Ar laser emitting $\sim 1W$ at 514.5 nm wavelength was used to photogenerate electron-hole pairs. These pairs subsequently decay nonradiatively and will be trapped by surface states, or recombine, due to a strong optical absorption on the surface.

Two undoped semi-insulating GaAs samples were used in these studies. The bulk electrical properties of both samples are controlled by the EL2 defect. One sample was untreated, while the other was chemically etched, followed by sulfur pretreatment with subsequent coating with a siloxane-type self-assembled-monolayer of thickness about 10 \AA .¹⁰ The surface photovoltage (SPV) measurement shown in Figure 1a clearly

indicates that the passivation has effectively tilted the surface band bending upward, resulting in an increase of the SPV signal. This is confirmed by an increased PL signal in the passivated sample at $T = 15 \text{ K}$ as shown in Figure 1b. The upward surface band bending will degrade the nonradiative recombination path on the surface by forcing the excess electrons to drift to the bulk regime. These excess electrons will then radiatively decay in the bulk at cryogenic temperatures. (The lower energy peak in the PL spectra is due to a carbon-related free-to-bound (e, C) emission, while the higher peak is due to a bound exciton-pair emission).

Results and discussion

In Figure 2, we show the PTR-DLTS spectra for both samples along with their Arrhenius plots. Within pulse repetition periods from $10 \mu\text{s}$ to $30 \mu\text{s}$, the untreated sample produces PTR-DLTS peaks that move from higher to lower temperatures as the repetition period increases. Therefore, the time constant responsible for these peaks *increases* as temperature *decreases*.⁸ This behavior is characteristic of a thermal emission process, opposite to a thermal capture process. The latter is often insensitive to temperature, or its time constant increases with increasing temperature. The position of each peak is determined by a polynomial fit of fourth order around the curve minimum for each curve of Figures 2a and 2b. The Arrhenius plot created from these peaks of the untreated sample gives an activation energy of $0.27 \pm 0.01 \text{ eV}$. The passivated sample, meanwhile, only produces peaks when the pulse repetition periods are set from $30 \mu\text{s}$ to $100 \mu\text{s}$. These peaks yield an activation energy of $0.26 \pm 0.02 \text{ eV}$. These two activation energies are remarkably close, and they are quite reproducible. In

Figure 3, the PTR transients from both samples clearly show that the passivated sample exhibits an increased time constant for $t \geq 5 \mu\text{s}$ after the excitation light cessation. (The excitation light consists of periodic square-wave pulses of 50% duty cycle). This is confirmed by the longer pulse repetition periods required to produce the PTR-DLTS peaks in the passivated sample. The after-the- "knee" long-time slopes calculated from Figures 3a and 3b are, respectively: $0.17 \text{ mV}/\mu\text{s}$ and $0.012 \text{ mV}/\mu\text{s}$. The identical activation energies obtained for both samples indicate that the excess carrier decay mechanism in both samples is controlled by the same surface native defect for the pulse repetition periods considered.

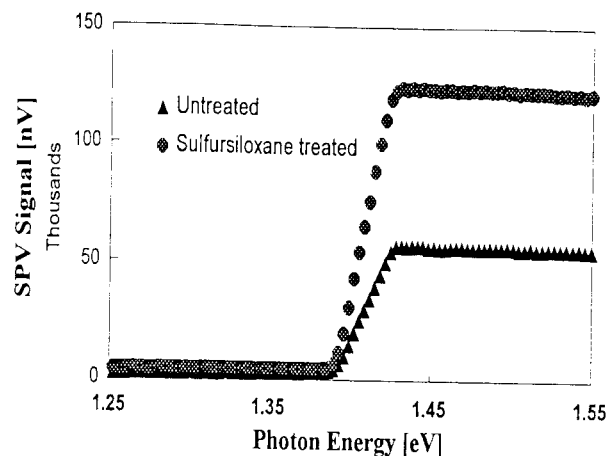


Figure 1a

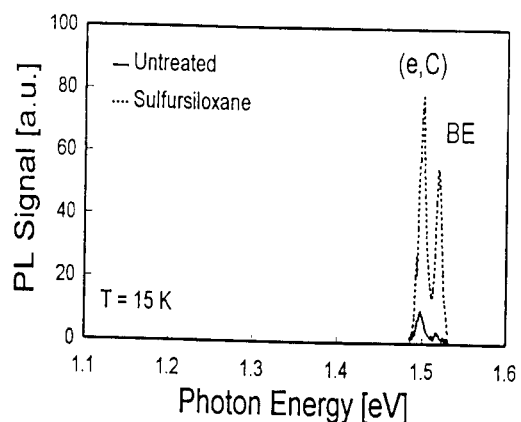


Figure 1b

Figure 1: a) Surface photovoltage and b) Photoluminescence spectra of untreated and passivated GaAs samples.

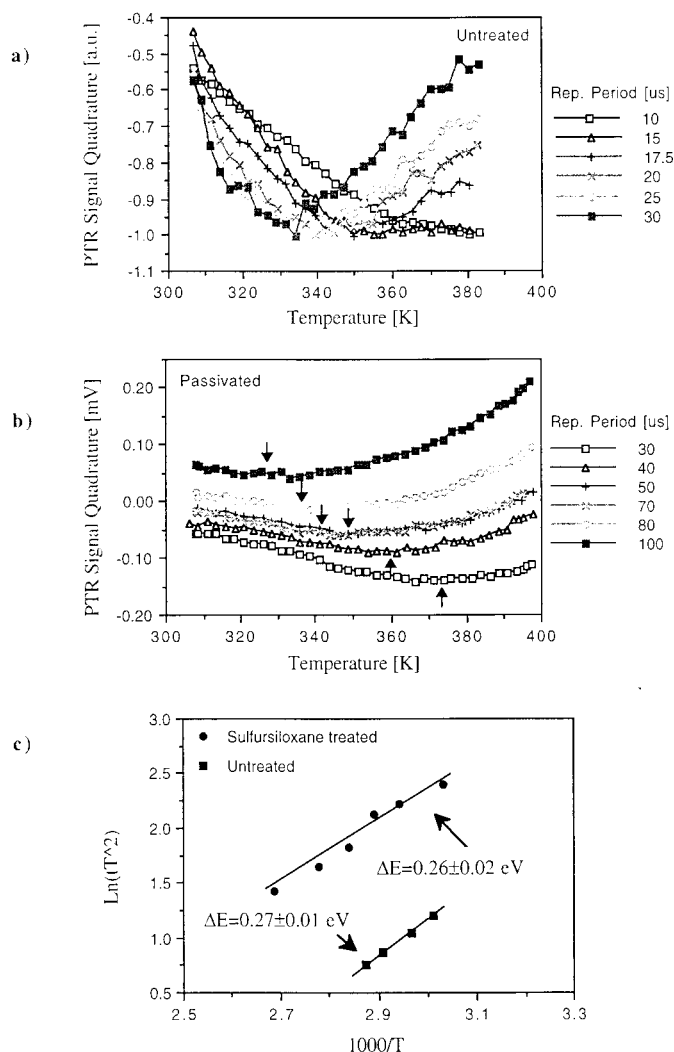


Figure 2: Photothermal radiometric deep level transient spectra (PTR-DLTS) for a) untreated and b) passivated GaAs samples. Also, shown are c) the Arrhenius plot for each sample. These yield activation energies of 0.27 ± 0.01 eV and 0.26 ± 0.02 eV for the untreated and passivated samples, respectively. PTR-DLTS spectra obtained here are from the quadrature channel of the lock-in amplifier. The positions of the broad minima in Figure 2b are indicated by arrows. The minima in (a) and (b) were determined using fourth-order polynomial fits.

We cannot assign this process to a surface nonradiative capture event that leads to a surface recombination event since: 1) the activation energy is not affected by a surface passivation which clearly changes the surface band bending, as can also be inferred from our SPV and PL results¹¹; and 2) the decay time constant for a nonradiative capture would occur at much shorter time scale commensurate with the excess carrier lifetime in semi-insulating GaAs. Moreover the observed microsecond decay time constant appears to be inconsistent with bulk-defect-controlled mechanisms, such as processes involving the EL2 center, that occur in the millisecond regime.¹²

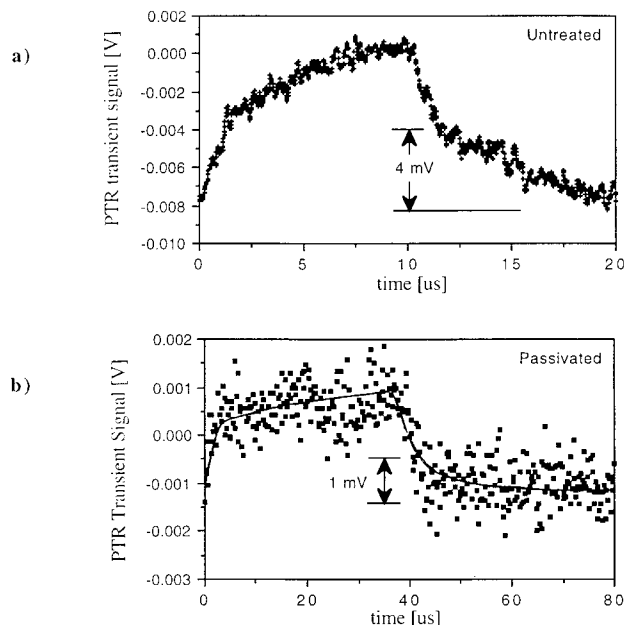


Figure 3: Photothermal radiometric (PTR) transients from a) untreated and b) passivated GaAs samples. The excitation light source is a periodic square wave pulse with repetition periods of 20 μ s and 80 μ s, respectively, and 50% duty cycle (ratio of pulse width to repetition period). The reduced PTR decay amplitude in the passivated sample indicates a longer decay time constant. A solid line representing the mean values of the transient in Figure 3b has been drawn to aid the eyes.

Thus, we attribute the 0.27 eV activation energy to carrier emission from a surface state. It will be shown that this emission process corresponds to a hole emission from a surface acceptor to the valence band. The early fast transient decay shown in Figure 3 may therefore be due to an electron and/or hole capture event that precedes the carrier emission, since this decay time constant does not change appreciably in both samples.

To understand the increased time constant exhibited in the passivated sample, we suggest that hole accumulation on the surface reduces the hole emission rate from the acceptor states to the valence band. Upward surface band bending pushes the Fermi level closer to the valence band, which decreases the electron occupancy level of the acceptor. This will further reduce the hole emission rate from the acceptor, since it is less able to capture accumulating excess holes. Figure 4 shows the band configuration, including the movement of excess carriers inside the space charge layer. In this case, we neglect the contribution from surface donor(s) since they are not likely to participate in the hole transport process. The 2.4 eV photons generate excess carriers within a depth of about 110 nm from the sample surface. The space charge layer width for the passivated samples is approximately 10 μ m, while the space charger layer width for the

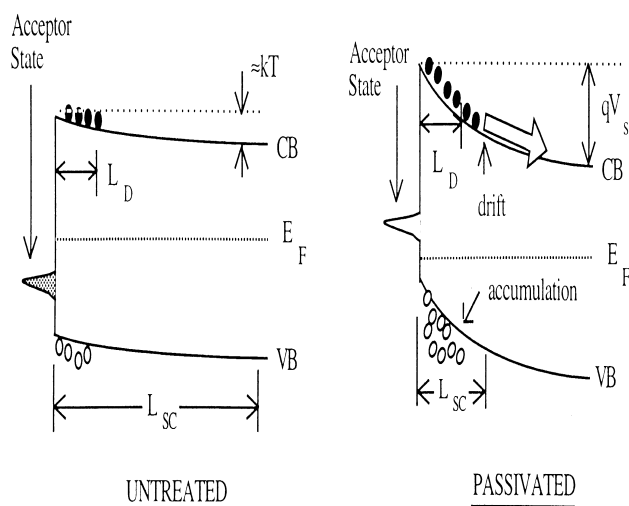


Figure 4: Proposed mechanism to explain the consistency of the 0.27 eV level and the apparent increase of the PTR decay time constant in the passivated sample. Excess carriers are captured within L_D , the ambipolar diffusion length from the surface, where the space charge layer width, L_{sc} , is one order of magnitude larger than L_D . Hence, few excess carriers are injected into the bulk. In addition, hole accumulation exists on the surface of the passivated sample due to an increased surface band bending. V_s is the barrier height introduced by passivation. The filled acceptor state represents a high electron occupancy level, while the hollow state represents a high hole occupancy level.

untreated sample is about $100 \mu\text{m}$.¹³ The narrower space charge layer width in the passivated sample is due to increased surface band bending. Therefore, most of the excess carriers will never reach the bulk region since the ambipolar diffusion length for undoped semi-insulating GaAs is typically about $1\text{-}2 \mu\text{m}$.¹⁴ While the excess electrons drift away from the surface, the excess holes will be spatially confined in the surface, driven by a more negative potential on the surface than in the bulk, and finally captured by surface acceptor states. This observation suggests that the hole transport is responsible for the PTR-DLTS peaks.

Based on the approximation $\tau \sim T_o$, we obtained an emission cross section of $\sigma_p \sim 10^{-16} \text{cm}^2$ at 350 K by using typical values for semi-insulating GaAs: thermal velocity of carriers $v_{th,p} \approx 10^7 \text{cm/s}$, and effective density of states in valence band $N_V \approx 10^{18} \text{cm}^{-3}$. This suggests that multiphonon emission process¹⁶ is the dominant carrier emission mechanism since another probable mechanism, i.e. cascade process, induces a much larger cross section.¹⁶

A numerical simulation of the PTR-DLTS spectrum was performed based on the carrier transport equation solution given by Chen *et al.*⁹ to test the assumption of $\tau \sim T_o$. We found that both values were of the same order of magnitude. The significance of this result comes from the fact that a cascade process assumes step like, discrete deep level impurities in the band gap, which is not very far from a continuum surface state configuration assumed in the MIGS model. Based on the foregoing arguments, we suggest that the defect-related mechanisms

as proposed by the AUDM or the DIGS model may be the dominant mode in pinning the Fermi level in undoped semi-insulating GaAs.

The activation energy we obtained coincides with the reported value for a V_{Ga} vacancy defect in the bulk region.¹⁷ Spicer *et al.*², however, assign the surface acceptor state to a Ga_{As} antisite defect in their AUDM model, while Hasegawa and Ohno³ attribute the acceptor state to the hybrid orbital energy of the sp^3 bond of the semiconductor. We have confirmed its energetic location from our PTR-DLTS results, but further physical analyses are needed to determine conclusively the physical nature of this acceptor state, which is still an open question at present.

Conclusions

In summary, we have shown that PTR-DLTS can reveal the theoretically predicted surface acceptor state in undoped semi-insulating GaAs, which is crucial in understanding the Fermi level pinning in this material. Our results support both the AUDM and the DIGS models which allow multiphonon emission transition for the electron energy dissipation. We also show that it is possible to observe carrier emission processes by the photothermal radiometric DLTS technique, an exciting development for this newly introduced analytical methodology.

Acknowledgements

We gratefully acknowledge the support of Materials and Manufacturing Ontario (MMO) through an Enabling Research Contract. One of us (R.A.B.) is grateful to the Office of Assessment and Application of Technology, Indonesia, for financial support.

References

- ¹W. Mönch, *Semiconductor Surfaces and Interfaces* (Springer, Berlin, 1995), p. 357.
- ²W.E. Spicer, Z. Lilienthal-Weber, E. Weber, N. Newman, T. Kendelewicz, R. Cao, C. McCants, P. Mohowald, K. Miyano, and I Lindau, *J. Vac. Sci. Technol.* **B6**, 1245 (1988).
- ³H. Hasegawa and H. Ohno, *J. Vac. Sci. Technol.* **B4**, 1130 (1986).
- ⁴J. Tersoff, *Phys. Rev. Lett.* **52**, 465 (1984).
- ⁵W. Mönch, *Surf. Sci.* **299/300**, 928 (1994).
- ⁶Ch. Hurtes, M. Boulou, A. Mitonneau, and D. Bois, *Appl. Phys. Lett.* **32**, 821 (1978).
- ⁷R.D. Fairman, F.J. Morin, and R. Oliver, in *Gallium Arsenide and Related Compounds 1978*, (IOP, London, 1979).
- ⁸A. Mandelis, R.A. Budiman, M. Vargas, and D. Wolff, *Appl. Phys. Lett.* **67**, 1582 (1995).
- ⁹Z.H. Chen, R. Bleiss, A. Mandelis, A. Buczkowski, and F. Shimura, *J. Appl. Phys.* **73**, 5043 (1993).
- ¹⁰I.P. Koutzarov, H.E. Ruda, L.Z. Jedral, C. Edrissinghe, Q. Liu, and R. Nicholov (to be published).
- ¹¹S.R. Dhariwal and D.R. Mehrotra, *Solid State Electron.* **31**, 1355 (1988).
- ¹²S. Makram-Ebeid, P. Langlade, and G.M. Martin, in *Semi-*

Insulating III-V Materials, edited by D.C. Look and J.S. Blakemore, 194 (Shiva, Cheshire, 1984).

¹³See, for example, the calculations in Reference 6, Ch. 2.

¹⁴Q. Liu, G. Chen, and H.E. Ruda, *J. Appl. Phys.* **74**, 7492 (1993).

¹⁵C.H. Henry and D.V. Lang, *Phys. Rev.* **B15**, 989 (1977).

¹⁶M. Lax, *Phys. Rev.* **119**, 1502 (1960).

¹⁷H.Q. Xu, and U. Lindefelt, *Phys. Rev.* **B41**, 5979 (1990).